Bulg. J. Phys. **34** (2007) 273–279

The Phase and Damping Effects on ATIR at Large Angles of Incidence

H.Y. Stoyanov

Department of Quantum Electronics, Faculty of Physics, University of Sofia, 5 J. Bouchier Blvd., 1164 Sofia, Bulgaria

Received *19 December 2007*

Abstract. A recently proposed [1] shearing interferometer can be applied in the study of the attenuator tilt effect on the amplitude and phase distribution in the totally reflected field. The liner variation of the separation between the prism boundary and the attenuator face causes, especially at larger angles of incidence, specific distribution of the phase shift between the p- and s-components of the reflected field. The interferometer allows to determine this shift by measuring the fringe intensity distribution along the aperture of the beam. An experiment with a glass prism – air – plane silicon attenuator is described. The results are compared with the theoretical predictions. For angles of incidence larger than the critical one a good agreement between theory and experiment was observed.

PACS number: 42.25.Gy, 07.60.Ly, 42.25.Ja, 78.68.+m, 42.25.Bs

1 Introduction

The attenuated total internal reflection (ATIR) offers a great variety of useful applications. It can be used for creating fixed or variable phase retarders [2-4], variable filters [5], in refractometry of optical materials such as absorbing liquids [6-9], metals, biotissue [10], forming of subwavelength surface relief [11], *etc*. Many experimental works in this field, mainly in the region of the longer wavelengths [12] have been carried out so far. The interferometers as precise phase handling tools gave us [1] the possibility to move the measurements in the visible range bringing up in the same time the research on a higher level of accuracy.

In the present paper further new results obtained with this interferometric method are described. The initially supposed plane parallel structure of the resonant three-layer system is only a mathematical abstraction. The keeping of this condition is very hard problem especially when the two physical bodies, the TIR prism and the attenuator, are adjusted each to other. In any case a small residual wedge will be observed. This nonparalelism leads to interesting effects at large

angles of incidence. These effects are easily detectable due to the high sensitivity of the interferometric phase meter. In addition, a recently described method [14] based on the reduced Rayleigh integral equation allows us to study the ATIR reflected field in the case of curved attenuator. The present work demonstrates that in the case of a system composed of almost plane boundaries and when the for attenuator is slightly inclined against the TIR boundary (Figure 2) the simpler matrix method gives sufficiently good results.

2 The Optical Setup

In the present report we are following the same way of study of the process of TIR attenuation and the same optical setup as that described in [8]. The optical system used in the experiment is shown in Figure 1. The laser source 'L' emits a linearly polarized beam, which is expanded and collimated by the collimator 'K'. The plane wave so obtained propagates through the 'TIR' prism 'PR'. The glass prism and the attenuator are mounted on a precise rotating stage 'RS'. The polarization beam splitter 'R' followed by the linear polarizer 'Pol', compose a simple shearing interferometer which allows us to study the phase shifts between the basic polarization components and their amplitude changes. The interferometric fringes are detected by a linear array image sensor 'Det' and analyzed by a PC-AT compatible computer. All elements are mounted on a vibration-isolated optical table.

Following the classical way [16] of study of the process of TIR we regard the incident and the output fields as compositions of two independent fields: the p-

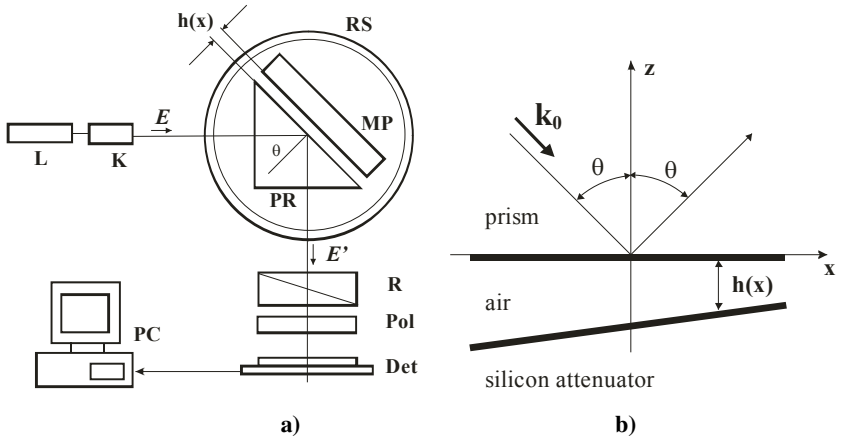

Figure 1. **a)** Sketch of the equipment: L – laser source, K – collimator, PR – glass prism, MP – metal plate, RS – rotating stage, R – Rochon prism, Pol – linear polarizer, Det – photodiode array detector, PC – personal computer with a framegraber; **b)** The geometry of the three-layer system.

and s-polarized components. Denoting by $\boldsymbol{S}(S_0, S_1, S_2, S_3)$ the Stokes vector of the incident field $\boldsymbol{E}$ (Figure 1), the Stokes vector $\boldsymbol{S}'(S_0', S_1', S_2', S_3')$ of the output ATIR field $\boldsymbol{E}'$ is given by the matrix equation [13]

$$\boldsymbol{S}' = \boldsymbol{M}_{\text{ATIR}} \cdot \boldsymbol{S}\,, \tag{1}$$

where $\boldsymbol{M}_{\text{ATIR}}$ is the Mueller matrix of the ATIR system. This matrix has the form [13]

$$\boldsymbol{M}_{\text{ATIR}} = \begin{bmatrix} m_{11} & m_{12} & 0 & 0 \\ m_{21} & m_{22} & 0 & 0 \\ 0 & 0 & m_{33} & m_{34} \\ 0 & 0 & m_{43} & m_{44} \end{bmatrix} \tag{2}$$

and its elements are functions [1,8] of all optical parameters of the system. We suppose constant and homogeneous optical properties of the glass prism, the intermediate space and the attenuating medium. Then the reflected field will be mainly dependant on the angle of incidence θ and on the gap width $h(x)$.

The intensity distribution of the output interferometric signal depends on the behavior of the output Stokes parameters and can be expressed in the form [1,8]

$$I(\boldsymbol{r}) = \frac{1}{2}\left\{S_0' + S_1' \cos 2\gamma + \left[S_2' \cos \Phi(x, \Delta) + S_3' \sin \Phi(x, \Delta)\right] \sin 2\gamma\right\}, \tag{3}$$

where the phase term $\Phi(x, \Delta)$ has the form

$$\Phi(x, \Delta) = (\boldsymbol{k}_p - \boldsymbol{k}_s) \cdot \boldsymbol{r} + \frac{2\pi}{\lambda} d(x)\Big[n_0 - \frac{n_e(\beta)}{\cos(\beta)}\Big] + \Delta,$$

where $\Delta = \delta_p - \delta_s$ is the phase difference between both components, β is the angle deviation between the ordinary and the extraordinary rays at the exit of the Rochon prism (the angular shear), γ is the azimuth of the polarizer (measured from the plane of incidence), $d(x)$ is the current thickness of the second right angle prism of the Rochon prism, $\boldsymbol{r}$ is the radius vector of the current point of measurement. In our case it lays in $0xz$ plane, $\boldsymbol{k}_p$, $\boldsymbol{k}_s$ are the wave vectors of the ordinary and extraordinary waves, which are corresponding to the *p*- and s-components of the ATIR field, respectively.

The numerical model of the Mueller matrix and of the Eq. (3) involves the gap thickness variations and allows predicting the intensity distribution in the output interferometric signal along the axes of the linear sensor for various combinations of optical materials and for any polarization state of the incident wave. Even the case of absorbing intermediate medium [7,17] can be studied in this way. In Figure 2 is shown the theoretical fringe intensity distribution along the aperture of the linear sensor as a function of the angle of incidence θ_3 for the media used in the following experiment (silicon mono-crystal $n_1 = 3.83 - i0.02$, air $n_2 = 1$, BaK4 glass $n_3 = 1.56687$).

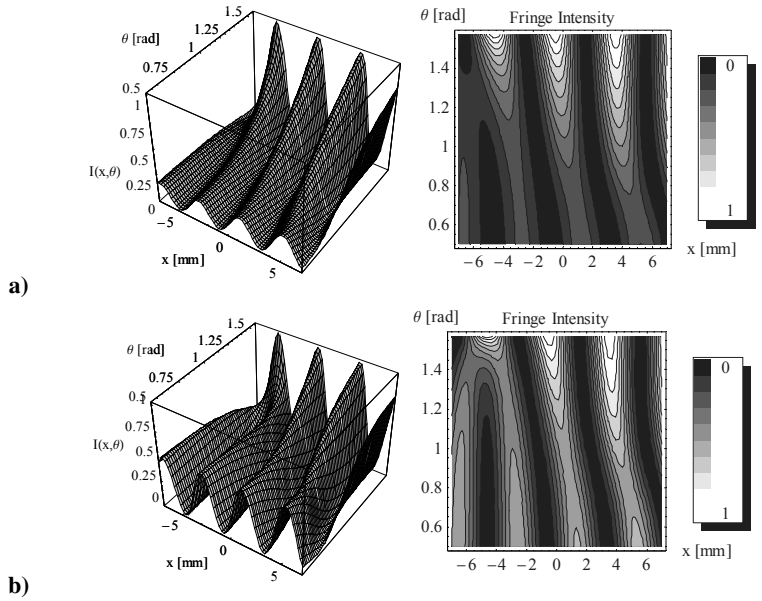

Figure 2. The theoretical fringe intensity distribution for: **a)** silicon mono-crystal attenuator ($n_1 = 3.83 - i0.02$ at $\lambda = 632.8$ nm [15]), **b)** evaporated chromium ($n_1 = 3.58 - i4.365$ at $\lambda = 632.8$ nm [18]), and for $n_2 = 1$ (Air), $n_3 = 1.56687$ (*Schott Jena* BaK4 at $\lambda = 632.8$ nm).

3 Experimental Results and Discussions

The source of linearly polarized coherent light in Figure 1 is a HeNe laser (*Melles Griot*, 3 mW), working in TEM_{00} mode. The beam is expanded and collimated up to approximately 50 mm dia. by a well corrected collimator (*Jodon*, model BET–50). From the so generated plane wave only a small part was used – approximately 2×15 mm in the central area of the aperture. The prism 'PR' was made of optical glass BaK4 (*Schott Jena*) with $n_3 = 1.56687$ at $\lambda = 632.8$ nm. The polarization interferometer consists of a Rochon prism and sheet linear polarizer. The Rochon provides an angular shear β of about 1.77×10^{-4} rad, so that only approximately four fringes cover the full aperture of the sensor. The photodiode array image sensor (*Matsushita*, model MN-512K) with 512 elements was used to detect photometric sections trough the interferometric fringes. The sensor pixel dimensions are 28×16 μm and the pitch is 28 μm. The total length of the sensitive area is 14.3 mm. The ADC-converter of the slot card framegraber provides 8 bits quantization of the video signal.

Special attention has been paid to the determination of the angle of the wedged gap. This measurement was carried out visually (in a manner similar to the

described in [1]) by means of measuring microscope (not shown in Figure 1) with long working distance lens (about 122 mm). The white light Fizeau fringes were observed in direction approximately normal to the hypotenuse of the TIR prism. The tilt was accomplished by a tree point micro screw adjusting stage mounted on the rotating table. The sample was fixed by spirituous solution of shellac. At the beginning the sample was adjusted by the three micro screws to almost parallel position against the plane of the TIR prism (infinite wide Fizeau fringe). From this initial situation the sample was rotated step by step around a vertical axis and the movement and the width of the dark brown-yellow fringe ($\lambda = 419$ nm approximately) was registered by the microscope. Additional correction of the value of the wedge angle due to the influence of through the prism observation was carried out. The wedge angle value was chosen to be approximately 10^{-5} rad. The reason for this was the observation that even at tiny inclinations (about 2 arcs of second in our case) the large angles of incidence lead to rapid changes in the fringe intensity distribution.

The angle of incidence has been measured and adjusted by a precise rotating stage (*Standa*, Model 7R7) which offers two scales of reading, coarse with resolution 1° and fine with resolution 1 arc minute. An optically polished plate of silicon mono-crystal, N-type, cut at (1,0,0) ($n_1 = 3.85 - i0.02$ at $\lambda = 632.8$ nm [15]) was used as attenuator. The intermediate space was filled with air. The array sensor allows us to capture and register almost linear photometric sections of the fringe intensity distribution shown in Figure 2. The results of the experiment shown in Figure 3 are four intensity sections measured for different angles of incidence.

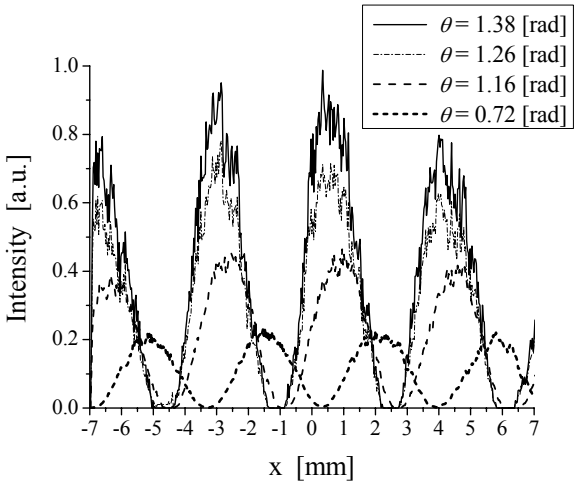

Figure 3. The experimental fringe intensity distribution measured at four different angles of incidence. The critical angle of incidence is $\theta_{3Critical} = 0.6926$ rad.

For angles of incidence exceeding the critical one the interferometer forms in the input pupil of the sensor approximately four full fringes. The increase of the angle of incidence leads to a progressive one side shift of the fringes together with the expectable raising of the overall intensity of the reflected field. The side shift progressively slows down and fringes formed at the angles of incidence in the range $(1.25, 1.138)$ rad have quite stable topography. The experimental results shown in Figure 3 are in a quite good agreement with the numerically predicted intensity distribution for the situations when the intermediate space is filled with air.

4 Conclusion

The comparison of the here described with the results for a plane parallel structure [1] leads to the following conclusions.

The wedge profile of the second medium causes monotonic and progressive shift aside of the interferometric fringes. There are no saddles in the intensity profile provided that the medium in the gap is perfect dielectric. The more complicated case when this medium is absorbing will be described in a separate paper.

The character of fringe contrast distribution for the case with presence of tilt is different compared with the same for plane parallel structure. This distribution is strongly dependant on the optical properties of the damping medium. For comparison this fact is illustrated on the case of chromium attenuator, Figure 2b. The numerical comparison of the evolution of the fringe intensity for silicon and chromium (at the same other conditions) shows the significance of the weight distribution of the value of the complex index of refraction between its components: the index of refraction n and the extinction coefficient κ. If the value of κ increases and that of n remains approximately the same, two effects are observed: a splitting in the intensity profile for large angles of incidence and progressive lateral shift of the fringes. The common conclusion is that higher values of the extinction coefficient lead to higher nonlinearity of the output interferometric signal.

The here described interferometric method proved to be a successful tool for ATIR phase investigation. The experiment gave results in good agreement with theory. The method can be used with success in the research and in other applications like the sensor technique, refractometry of absorbing media, contamination monitoring, *etc*.

Acknowledgments

This work was supported by the National Science Fund of Bulgaria, grant No. VUF-02-05.

References

[1] H.Y. Stoyanov (2000) *Opt. Laser Technol.* **32** 147.
[2] A.M. Kan'an, R.M.A. Azzam (1994) *Opt. Eng.* **33** 2029.
[3] E. Cojocaru (1994) *Appl. Optics* **33** 7425.
[4] E. Spiller (1984) *Appl. Optics* **23** 3544
[5] Yu. Wang (1995) *Appl. Phys. Lett.* **67** 2759.
[6] W. Wild (1982) *Phys. Rev. A* **25** 2099.
[7] H.Y. Stoyanov (2006) *Bulg. J. Phys*. **33** 25.
[8] H.Y. Stoyanov (2007) *Opt. Laser Technol*. **39** 885.
[9] M. McClimans, C. LaPlante, D. Bonner, S. Bali (2006) *Appl. Opt*. **45** 6477.
[10] H. Li, Sh. Xie (1996) *Appl. Opt.* **35** 1793.
[11] J.C. Martinez-Anton (2006) *J. Opt. A: Pure Appl. Opt*. **8** S213.
[12] W. Culshow, D.S. Jones (1953) *Proc. Phys. Soc.* **B66** 859.
[13] E. Collett (1993) *Polarized Light. Fundamentals and Applications*, Marcel Dekker, New York.
[14] Z.D. Genchev, H.Y. Stoyanov (2005) *Appl. Phys. B* **81** 657.
[15] R.M.A. Azzam (1985) *Appl. Optics* **24** 513.
[16] M. Born, E. Wolf (1959) *Principals of Optics*, Pergamon Press, London.
[17] H.Y. Stoyanov (2007) *Proc. SPIE* **6604** 66040R.
[18] E.D. Palik (1985) *Handbook of Optical Constants of Solids*, Academic Press, New York.